

The environment of low redshift quasar pairs.

A. Sandrinelli^{1,2,3*}, R. Falomo⁴, A. Treves^{1,2,3}, E. P. Farina⁵, M. Uslenghi⁶

¹ *Università degli Studi dell'Insubria, Via Valleggio 11, I-22100 Como, Italy*

² *INAF - Osservatorio Astronomico di Brera, Via Emilio Bianchi 46, I-23807 Merate, Italy*

³ *INFN - Istituto Nazionale di Fisica Nucleare, Sezione Milano Bicocca,*

Dipartimento di Fisica G. Occhialini, Piazza della Scienza 3, I-20126 Milano, Italy

⁴ *INAF - Osservatorio Astronomico di Padova, Vicolo dell'Osservatorio 5, I-35122 Padova, Italy*

⁵ *Max Planck Institut für Astronomie, Königstuhl 17, 69117 Heidelberg, Germany*

⁶ *INAF-IASF - via E. Bassini 15, I-20133 Milano, Italy*

Accepted – Received –

ABSTRACT

We investigate the properties of the galaxy environment of a sample of 14 low redshift ($z < 0.85$) quasar physical pairs extracted from SDSS DR10 archives. The pairs have a systemic radial velocity difference $\Delta V_{\parallel} \leq 600 \text{ km s}^{-1}$ (based on [OIII]5007 Å line) and projected distance $R_{\perp} \leq 600 \text{ kpc}$. The physical association of the pairs is statistically confirmed at a level of $\sim 90\%$. For most of the images of these quasars we are able to resolve their host galaxies that turn out to be on average similar to those of quasars not in pairs. We also found that quasars in a pair are on average in region of modest galaxy overdensity extending up 0.5 Mpc from the QSO. This galaxy overdensity is indistinguishable from that of a homogeneous sample of isolated quasars at the same redshift and with similar host galaxy luminosity. These results, albeit derived from a small (but homogeneous) sample of objects, suggest that the rare activation of two quasars with small physical separation does not require any extraordinary environment.

Key words: galaxies: clusters, general– quasars, general, quasar pairs.

1 INTRODUCTION

It is widely accepted that all massive galaxies contain a supermassive black hole in their centers. However, only a small fraction of them become active and for a very short time with respect to the evolution time of the galaxies. The mechanism that activates and fuels the nuclei of galaxies is still not well understood. The leading processes thought to be responsible for transforming a dormant massive black hole into a luminous quasar (QSO) are dissipative tidal interactions and galaxy mergers (e.g. Di Matteo, Springel, & Hernquist 2005; Callegari et al. 2011, and references therein). Galaxy formation is known to be heavily influenced by the environment, with galaxies in clusters tending to be elliptical and deprived of most of their gaseous content (e.g. Silk & Wyse 1993; Kormendy et al. 2009), and in a number of cases showing signature of interactions and mergers (e.g. Bennert et al. 2008; McIntosh et al. 2008). What is the effective role of these interactions and of the large scale environment for the triggering and/or fuelling the nuclear activity is not yet clear.

The investigation of QSO environments at various scales

(from few kpc to Mpc) and at different cosmic epochs compared with that of normal galaxies still represents an important opportunity to unveil the link between nuclear activity and the immediate environment. The studies of galaxy clustering around quasars (Stockton 1978; Yee & Green 1984, 1987) and other active galaxies (e.g. Wake et al. 2004) aim to characterize the properties of the environment and to compare them with the environment of non active galaxies. The emerging picture is not homogeneous. Most of the papers conclude that quasars reside in regions of galaxy density that are higher than average, albeit with significant difference among various objects. Only in rare cases quasars are found in relatively rich environments (Stockton 1978; Yee & Green 1984) and the typical environment is a modest group or a poor cluster of galaxies.

Contrasting results emerge when the quasar environments are compared with those of non active galaxies, depending on the properties of the sample (nuclear luminosity, redshift, radio loudness, ect.). Some differentiation emerges from the comparison of radio loud and radio quiet quasars. Ellingson et al. (1991) studied a sample of radio loud quasars (RLQs) and radio quiet quasars (RQQs) at $0.3 < z < 0.6$ and found that the environments around RLQs are significantly denser than those around RQQs.

* E-mail: asandrinelli@yahoo.it / angela.sandrinelli@brera.inaf.it

However, Fisher et al. (1996) and McLure & Dunlop (2001) find no difference between the environments of RLQs and RQQs. More recently from the analysis of a large QSO dataset at $z < 0.4$ from Sloan Digital Sky Survey (SDSS) Serber et al. (2006) found that the overdensity around the quasars is larger than that around typical L* galaxies. However, a more complete comparison of quasars and inactive galaxies environments by Karhunen et al. (2014), that includes a matching of the samples in terms of both redshift and galaxy luminosity, shows that the galaxy number density of the quasar environments is comparable to that of the inactive galaxies.

Another important issue about the environment of quasars is that they are found clustered similarly to galaxies in the local Universe (e.g. Croom et al. 2005; Porciani, Magliocchetti, & Norberg 2004, and reference therein). At high redshift the clustering is more difficult to measure but there are indications that its strength would be higher than at the present epoch (e.g. Porciani, Magliocchetti, & Norberg 2004). The clearest sign of QSO clustering is the finding of quasar pairs, see e.g. the pioneering work of Djorgovski 1991 and the analysis on the Veron-Cetty & Veron (2000) catalogue by Zhdanov & Surdej (2001). Hennawi et al. (2006) found a large sample of QSO pair candidates in a wide range of redshift but a detailed study of the environment was not carried out. Most of these QSO pairs ($\sim 80\%$) are at $z > 1$ hindering observations of their environment. A number of high redshift QSO pairs have also been discovered by Hennawi et al. (2010).

Detailed study of the environment of a QSO pair at $z \sim 1.3$ has been reported by Djorgovski et al. (1987). Boris et al. (2007) investigated the environment of 4 QSO pairs at $z \sim 1$ with separations $\gtrsim 1$ Mpc. They found one pair in a particularly high-density region, some evidences for galaxy cluster in the proximity of other two, while one pair appears isolated. A more systematic study was presented by Farina, Falomo, & Treves (2011) (hereafter F11) for six low redshift physical quasar pairs from the SDSS dataset. They reported a pair in a moderately rich group of galaxies together with dynamical evidence of additional mass to make the pairs bound systems. More recently Green et al. (2011) searched for signatures of galaxy clusters and hot inter cluster medium associated with 7 close ($R_{\perp} < 25$ kpc) quasar pairs. Because of low quality images they fail to resolve the host galaxies and to set stringent limits to the galaxy environments. Nevertheless from their observations there is no evidence that these pairs are in rich cluster environments.

Rare examples of quasar associations with more than two objects have been reported (Djorgovski et al. 2007; Farina et al. 2013) but the limited number prevents to perform a statistical analysis.

In this paper we explore the galaxy environments and the dynamical properties around 14 low redshift quasar physical-pairs derived from SDSS Data Release 10 (DR10) spectroscopic and imaging datasets. For these systems we perform a detailed analysis of their host galaxies and of the clustering of galaxies around the pairs. We are then able to compare the properties of these environments with those of an homogeneous sample of quasars not in pair spanning the same range of redshift and host galaxy luminosities. Finally from the difference of systemic velocity of each pair (derived

from [OIII] λ 5007 emission lines, hereafter [OIII]) we set constraints on the total minimum mass of the systems based on the dynamic of the pair.

In this work we assume a concordant cosmology: $H_0 = 70 \text{ km s}^{-1} \text{ Mpc}^{-1}$, $\Omega_m = 0.30$ and $\Omega_{\Lambda} = 0.70$.

2 THE SAMPLE OF QUASAR PHYSICAL PAIRS

We searched for quasar pair candidates from a dataset of $\sim 260,000$ quasars drawn from the SDSS combining the quasar spectroscopic catalogues of Schneider et al. (2010) and of Pâris et al. (2013). We restricted the search to the $\sim 40,000$ quasars with $z < 0.85$, in order to derive redshifts from [OIII] narrow emission line, which is a much better indicator of the systemic velocity of the quasar host galaxy (Hewett & Wild 2010; Liu et al. 2013).

To search for QSO pair candidates we computed the number N_{obs} of quasars in the catalogue that have $\Delta V_{\parallel} < \Delta V_{\parallel,limit}$ and $R_{\perp} < R_{\perp,limit}$, where $\Delta V_{\parallel,limit}$ and $R_{\perp,limit}$ are fixed values, and compared with the number N_{exp} of expected random association using the redshift permutation method (e.g. Zhdanov & Surdej 2001). It consists in maintaining fixed the positions of the quasars, permuting randomly the redshifts. 10,000 runs were performed. We repeated the search with various value of $\Delta V_{\parallel,limit}$ and $R_{\perp,limit}$ in order to optimize the number of candidates with respect to the number of chance associations. It turns out that the best choice is $R_{\perp} < 600$ kpc and $\Delta V_{\parallel} < 600 \text{ km s}^{-1}$. For this combination we find 26 QSO pair candidates of which only 3-4 ($\sim 14\%$) are expected to be false pairs (random associations).

At this stage of the selection ΔV_{\parallel} was determined from SDSS redshifts. We inspected the spectra of all candidates to ensure that the systemic ΔV_{\parallel} could be reliably derived from [OIII] lines. For two dubious classifications we removed two QSO pairs candidates, another one for the lack of the [OIII] wavelength region in one spectrum. Because of poor S/N, 8 pair candidates have the [OIII] line position hardly measurable for at least one quasar. For the remaining pairs the [OIII] line position was measured with procedure described in F11, where the centroid was evaluated as the median of the barycenters of the line above different flux thresholds and the interquartile range as uncertainty. In one case ΔV_{\parallel} from [OIII] did not satisfy the condition $< 600 \text{ km/s}$, which instead was fulfilled by the SDSS redshifts, and the pair candidate was removed.

In our sample of 14 QSO pairs we then expect that 1-2 pairs could be chance superpositions. We can assume that the selected sample is mostly composed of physically associated objects where the quasar velocities are due to gravitational binding. The final list of the quasar pairs candidates is reported in Table 1 and details on [OIII] line measurements are given in Table 2. None of our QSO pairs are present in catalogs of lensed quasars (CfA-Arizona Space Telescope LEns Survey of gravitational lenses, CASTLE¹; SDSS Quasar Lens Search, SQLS²). Moreover detailed com-

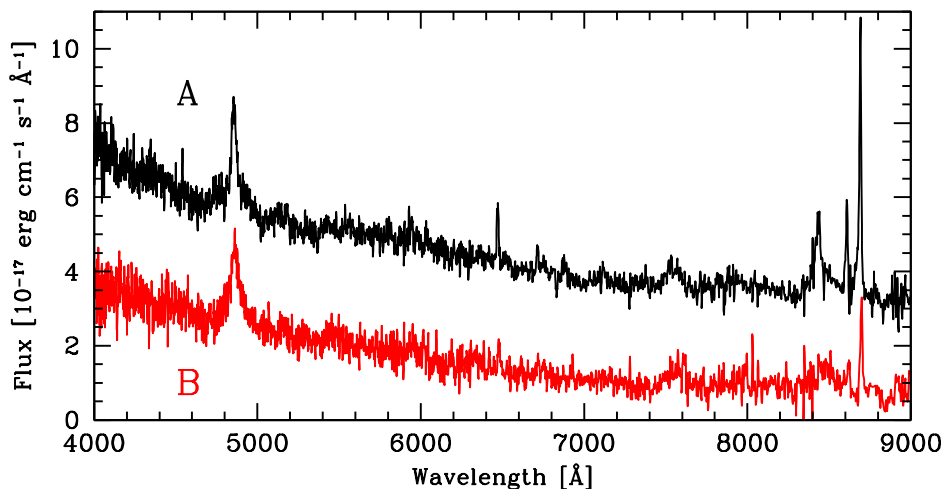
¹ <http://www.cfa.harvard.edu/castles/>

² <http://www-utap.phys.s.u-tokyo.ac.jp/~sdss/sqls/index.html>

Table 1. Properties of low redshift quasar pair sample.

Pair Nr	A	z_A	i_A [mag]	B	z_B	i_B [mag]	$\Delta\theta$ [arcsec]	R_\perp [kpc]	ΔV_\parallel [$km\ s^{-1}$]
(a)	(b)	(c)	(d)	(e)	(f)	(g)	(h)	(i)	(j)
1	J001103.18+005927.2	0.4865	19.75	J001103.48+010032.6	0.4864	20.62	652	390	19 ± 28
2	J022610.98+003504.0	0.4240	19.54	J022612.41+003402.2	0.4239	19.09	66.0	360	25 ± 24
3	J074759.02+431805.3	0.5011	18.84	J074759.65+431811.4	0.5017	19.09	8.9	60	123 ± 18
4	J081801.47+205009.9	0.2357	17.45	J081808.77+204910.1	0.2356	18.81	118.1	440	36 ± 16
5	J082439.83+235720.3	0.5353	18.71	J082440.61+235709.9	0.5368	18.61	15.5	90	294 ± 19
6	J084541.18+071050.3	0.5376	18.73	J084541.52+071152.3	0.5352	18.60	62.3	390	468 ± 51
7	J085625.63+511137.0	0.5420	18.38	J085626.71+511117.8	0.5432	19.18	22.5	140	148 ± 21
8	J095137.01-004752.9	0.6340	20.23	J095139.39-004828.7	0.6369	20.02	49.8	350	544 ± 23
9	J113725.69+141101.3	0.7358	20.03	J113726.12+141111.4	0.7372	20.53	12.4	90	238 ± 28
10	J114603.49+334614.3	0.7642	20.11	J114603.76+334551.9	0.7615	19.23	23.3	170	445 ± 38
11	J124856.55+471827.7	0.4386	18.62	J124903.33+471906.0	0.4386	18.30	79.4	450	4 ± 15
12	J133046.35+373142.8	0.8141	19.32	J133048.58+373146.6	0.8144	19.82	26.4	200	54 ± 43
13	J155330.22+223010.2	0.6413	18.22	J155330.55+223014.3	0.6422	20.65	5.9	40	175 ± 12
14	J222901.08+031139.8	0.8069	21.69	J222902.03+031024.7	0.8087	19.88	76.5	570	299 ± 19

Notes: (a) Pair identification number. (b); (e) SDSS quasar name. (c); (f) Quasar redshifts derived from [OIII] line positions. (d); (g) i-band apparent magnitude of the quasar A and B, respectively (h) Angular separation of the pair. (i) Proper traverse separation R_\perp . (j) Radial velocity difference.


Figure 1. SDSS spectra of the QSOs in pair nr. 9 at $z=0.736$. For clarity of comparison, the spectrum of the quasar A is shifted upwards.

parison between the spectra of each pair exhibits clear differences that exclude the possibility of gravitational lensing. The redshifts of these quasar pairs are $0.23 \lesssim z \lesssim 0.82$, with $z_{ave} = 0.58 \pm 0.16$. An example of the SDSS spectra of a selected QSO pair is given in Figure 1.

3 HOST GALAXIES

We retrieved the i-images of quasar pairs from the SDSS-DR10 imaging archive. Analysis was made using the Astronomical Image Decomposition and Analysis software (AIDA

Uslenghi & Falomo 2008). Our procedure for the study of the quasar host galaxies follows closely that adopted by Falomo et al. (2014) for the imaging study of 400 low redshift ($z < 0.5$) SDSS quasars in Stripe 82. In particular the analysis provides the decomposition of the quasar components, nucleus and host galaxy (see Figure 2), resulting in 19 quasars with resolved host galaxies (R), 5 marginally resolved (M), and 4 objects unresolved (U); for ten pairs we are able to characterize the host galaxy properties of either quasars. The measured i magnitudes (AB system) of the nucleus and of the host galaxy are reported in Table 3, together with the rest frame Vega M_R absolute magni-

Table 2. Measurements of [O III] λ 5007 Å emission lines based on the median of the baricenter of the line (see text).

Pair Nr (a)	$\lambda_{[\text{OIII}]}$ (A) [Å] (b)	$\lambda_{[\text{OIII}]}$ (B) [Å] (c)
1	7442.47 ± 0.63	7441.99 ± 0.26
2	7129.84 ± 0.44	7129.24 ± 0.32
3	7515.70 ± 0.26	7518.77 ± 0.30
4	6187.15 ± 0.24	6186.41 ± 0.22
5	7686.78 ± 0.37	7694.31 ± 0.26
6	7698.28 ± 0.30	7686.28 ± 1.27
7	7722.53 ± 0.47	7726.33 ± 0.20
8	8180.92 ± 0.06	8195.76 ± 0.61
9	8690.95 ± 0.33	8697.85 ± 0.70
10	8832.83 ± 1.10	8819.75 ± 0.04
11	7202.80 ± 0.05	7202.88 ± 0.32
12	9082.84 ± 0.41	9084.48 ± 1.22
13	8217.60 ± 0.26	8222.40 ± 0.07
14	9047.04 ± 0.37	9056.06 ± 0.39

Notes: (a) Pair identification number. (b); (c) Emission line centers of [O III] λ 5007 emission line for quasars A and B, respectively.

tude, dereddened and k-corrected. Corrections for galactic extinction were taken from SDSS database and k-corrections from templates of Mannucci et al. (2001) and Francis et al. (2001) for host galaxies and nuclei, respectively.

The average absolute magnitudes $M_R(\text{nuc})$ of the nuclei is -23.0 ± 1.1 (median -23.1 ± 0.7), similar to the nuclear luminosities of isolated quasars (e.g. Falomo et al. 2014). We find that the absolute magnitude $M_R(\text{host})$ of the host galaxies range between -21 and -24.5 (mean -22.9 ± 0.8 ; median -22.9 ± 0.5). The distribution of $M_R(\text{host})$ is comparable within similar redshifts to that reported for quasars that are not in pairs (Falomo et al. 2014), indicating that the two families of QSO (individuals and in pairs) are indistinguishable from this point of view. Note that for $\sim 60\%$ of the objects the observations in the i filter include the [OIII] emission line. This might contaminate the measurement of the host galaxy luminosity (e.g. because of scattered light from the nucleus). However, the same effect would be present also in the case of single quasars at similar redshifts.

4 GALAXY ENVIRONMENT OF THE QUASAR PAIRS

In order to characterize the QSO pair environments, we analyzed the distribution of galaxies around the quasars using SDSS DR10 catalogues. From these we obtained position and photometry of galaxies by selecting all primary objects photometrically classified as galaxies. In each quasar pair field, we analyzed the i -band surface distribution of the galaxies within a circular area of 15 arcmin radius, corresponding to a projected distance of 3.4 Mpc from the nearest pair ($z=0.236$) and 9.3 Mpc from the farthest ($z=0.807$).

To estimate the completeness of the SDSS galaxy catalogues we compared the differential number counts of detected galaxies as a function of the magnitude with the very

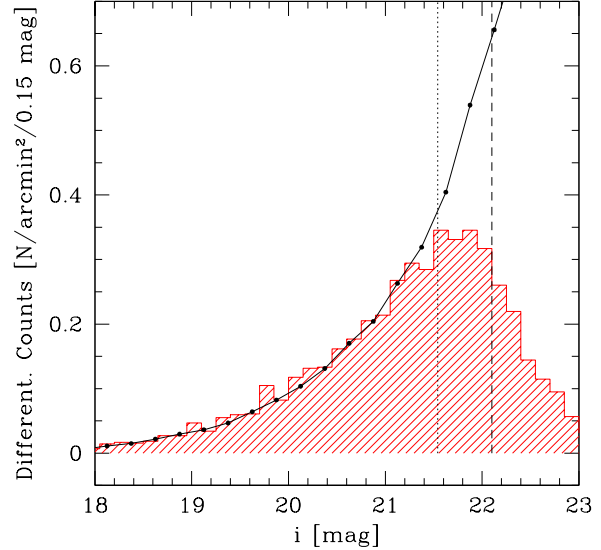


Figure 3. Number counts of galaxies as a function of i -magnitude in the field of QSO pair nr.2 (red shallow histogram). The black solid line represents for comparison the counts from deep survey of Capak et al. (2007). The dotted and dashed vertical lines mark the median magnitude and 50% completeness threshold.

deep galaxy count data available from the Durham University Cosmology Group³. In particular for each field we considered as threshold the magnitude $m_{i,50\%}$ where the completeness of observed galaxies drops to 50% of that expected from Capak et al. (2007) (see Figure 3).

The apparent i -magnitude thresholds are closely distributed around the mean value of 21.96 ± 0.09 and listed in Table 4 with the corresponding absolute k-corrected magnitudes. At these thresholds we can observe galaxies with magnitude M^*+2 at $z < 0.3$, M^*+1 at $z \lesssim 0.5$ and M^* at $z \lesssim 0.8$.

In order to study the galaxy environment we followed the procedure described by Karhunen et al. (2014). To evaluate the surface number density of galaxies in the background, n_{bg} , we considered the galaxies with $i < m_{i,50\%}$ and projected angular distance between 7 and 15 arcmin from the midpoint of the quasar pair. This corresponds to a minimum distance from the QSO of ~ 1.6 Mpc for the nearest target. The region was then divided into annuli with width of 1 arcmin and we compute n_{bg} as the median of the galaxy surface density of each annulus and the semi interquartile range is assumed as scatter (see Table 4). Finally for each QSO we counted the surface number density of galaxies in a number of annuli with width of 250 kpc around the target. The galaxy overdensity of the QSO environment is the ratio between this number density and that of the background. In order to take into account the contribution of galaxies in the field around the quasar pair in the case that the annuli around the two QSO are overlapping, we have subdivided the excess galaxies in common to an equal num-

³ Durham University Cosmology Group, references and data in <http://astro.dur.ac.uk/~nm/pubhtml/counts/counts.html>

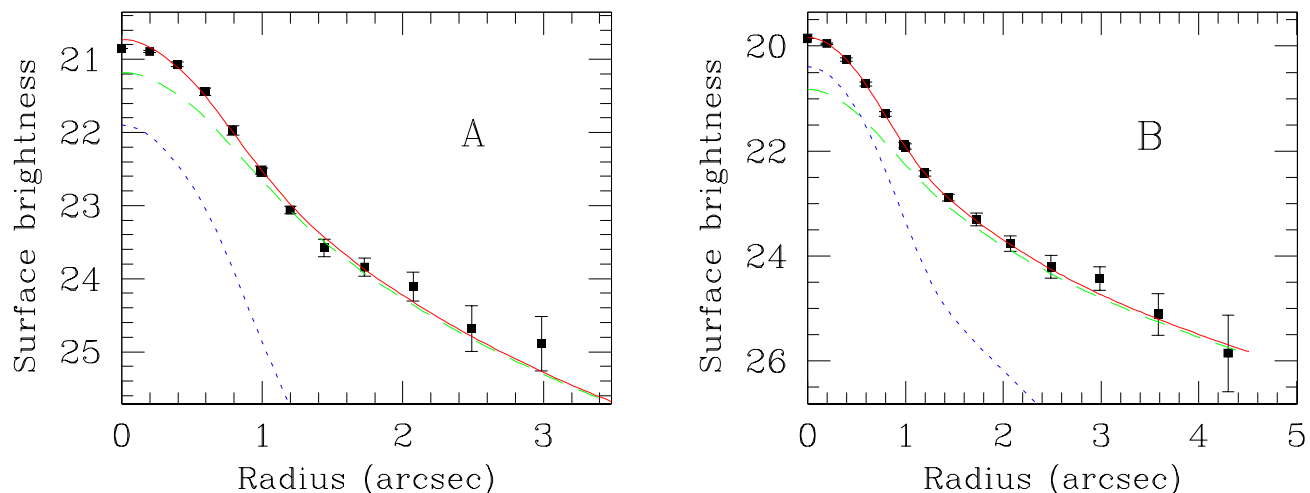


Figure 2. Examples of the quasar host galaxies decomposition for the QSO pair nr. 2. *Left panel:* Average radial brightness profile of the quasar A (square dots) fitted by the scaled PSF (blue dotted line) plus the the host galaxy model convolved with the PSF (green dashed line), see text. The best fit is represented by the red solid line. *Right panel:* The same for the quasar B.

Table 3. Properties of nuclei and host galaxies.

QSO ID	Class	i_{nuc} [mag]	i_{host} [mag]	$M_R(nuc)$ [mag]	$M_R(host)$ [mag]	M(host) [$10^{12} M_{\odot}$]
(a)	(b)	(c)	(d)	(e)	(f)	(g)
1A	R	19.90	21.61	-22.42	-21.07	0.09
1B	R	—	20.35	—	-22.33	0.3
2A	R	21.68	19.51	-20.38	-22.74	0.4
2B	R	20.16	19.03	-21.9	-23.22	0.7
3A	R	19.19	19.55	-23.23	-23.27	0.7
3B	R	19.45	19.90	-22.97	-22.94	0.5
4A	R	19.65	17.92	-20.64	-22.66	0.5
4B	R	19.29	19.68	-20.99	-20.90	0.09
5A	R	18.90	19.76	-23.65	-23.27	0.6
5B	M	18.77	20.43	-23.79	-22.61	0.4
6A	R	18.81	20.70	-23.74	-22.36	0.3
6B	M	18.72	20.53	-23.84	-22.51	0.3
7A	R	18.68	19.48	-23.86	-23.55	0.9
7B	U	19.17	—	-23.37	—	—
8A	R	20.50	19.98	-22.46	-23.64	0.9
8B	R	20.28	21.23	-22.7	-22.40	0.3
9A	U	20.08	—	-23.01	—	—
9B	R	21.32	21.03	-22.05	-23.15	0.5
10A	R	20.34	21.10	-23.13	-23.20	0.5
10B	R	19.25	19.69	-24.21	-24.59	1.9
11A	M	19.35	19.34	-22.75	-22.98	0.5
11B	U	18.31	—	-23.79	—	—
12A	M	19.43	21.01	-24.33	-23.51	0.7
12B	R	19.99	20.27	-23.66	-24.25	1.4
13A	R	18.29	20.04	-24.73	-23.65	0.9
13B	U	20.64	—	-22.39	—	—
14A	R	22.05	22.27	-21.75	-22.37	0.3
14B	M	19.99	21.97	-23.82	-22.68	0.3

Notes. (a) Quasar identifier. (b) Resolved (R), marginally resolved (M), unresolved (U). (c); (d) Apparent i-magnitude (AB system) of the nucleus and host galaxy. (e); (f) Absolute R-band magnitude (Vega system, k-corrected and dereddered) of the nucleus and host galaxy. (g) Mass of the host galaxy (see text).

Table 4. Statistics of galaxy in the QSO pair environments.

Pair Nr	$m_{i,50\%}$ [mag]	$M_{i,50\%}$ [mag]	n_{bg} [arcmin $^{-2}$]	n_{bg} [Mpc $^{-2}$]	$G_{0,5}(A)$	$G_{0,5}(B)$
(a)	(b)	(c)	(d)	(e)	(f)	(g)
1	21.9	-20.76	3.40 ± 0.10	26.20 ± 0.80	1.22 ± 0.04	0.68 ± 0.02
2	22.1	-20.14	4.01 ± 0.10	36.15 ± 2.71	1.14 ± 0.09	1.28 ± 0.10
3	21.9	-20.86	3.09 ± 0.16	23.16 ± 1.49	1.04 ± 0.12	1.04 ± 0.15
4	21.9	-18.62	2.24 ± 0.29	44.14 ± 6.02	0.89 ± 0.04	1.10 ± 0.04
5	21.9	-21.07	3.21 ± 0.09	22.30 ± 0.70	1.27 ± 0.07	1.21 ± 0.07
6	21.9	-21.08	3.27 ± 0.16	22.97 ± 1.39	0.87 ± 0.04	0.92 ± 0.07
7	21.8	-21.22	3.15 ± 0.15	21.98 ± 0.69	0.75 ± 0.15	0.87 ± 0.14
8	21.9	-21.67	3.06 ± 0.14	18.40 ± 0.59	1.11 ± 0.07	1.25 ± 0.05
9	22.0	-22.22	3.38 ± 0.16	17.85 ± 1.05	1.21 ± 0.04	0.93 ± 0.05
10	22.0	-22.41	3.41 ± 0.18	17.40 ± 1.02	1.27 ± 0.07	1.13 ± 0.07
11	22.0	-20.34	3.86 ± 0.10	33.88 ± 0.87	1.15 ± 0.04	1.07 ± 0.04
12	22.1	-22.68	4.56 ± 0.23	22.47 ± 0.98	0.88 ± 0.05	1.51 ± 0.06
13	22.0	-21.61	2.89 ± 0.27	17.05 ± 1.76	1.41 ± 0.02	1.33 ± 0.03
14	22.1	-22.63	4.10 ± 0.27	20.15 ± 1.47	0.57 ± 0.03	0.70 ± 0.03

Notes: (a) Quasar pair identification number. (b) Apparent SDSSi-magnitude threshold. (c) Absolute magnitude corresponding to $m_{i,50\%}$. (d); (e) Background surface number density of galaxies in arcmin $^{-2}$ and Mpc $^{-2}$, respectively. (f);(g) Galaxy overdensity in the region within 500 kpc from the QSO, see text.

ber for each quasars. The average cumulative overdensity distribution for the 28 quasars is reported in Figure 4, left panel, and compared with that of isolated quasars derived by Karhunen et al. (2014). We find that on average the galaxy overdensity around quasars in pair is indistinguishable from that of isolated quasars. For each QSO in our sample we report in Table 4 the galaxy overdensity inside a radius of 500 kpc.

It is of interest to probe whether the galaxy overdensity depends on the separation of the quasar pairs. To aim this we computed the galaxy overdensity of the six pairs that are separated by less than 180 kpc and compare it with that expected under the assumption that each individual QSO contributes to the average value of galaxies (as given in Figure 4, left panel). The comparison (see Figure 4, right panel) suggests that closest quasar pairs may be in richer environments than those at larger separation. We performed a KS test comparing the galaxy overdensity distribution of QSO pairs with $R_{\perp} < 180$ kpc to that of QSO pairs with larger separations. For the cumulative galaxy overdensity up to 1500 kpc the KS test yields the probability $p=0.08$. This indicates that the suggestion should be confirmed by a significantly larger sample.

5 SUMMARY AND CONCLUSIONS

We have investigated the properties of the environments of a sample of 14 physical low redshift QSO pairs. We found that the quasars in pairs are on average in regions of modest galaxy overdensity extending up to ~ 0.5 Mpc. This overdensity is indistinguishable from that of a homogeneous sample of isolated quasars (Karhunen et al. 2014) that is matched in redshift and host galaxy luminosity. We note that for the closest QSO pairs there is a suggestion of a larger overdensity roughly commensurated to the sum of the average individual quasar environments.

Although the number of known QSO pairs candidates (e.g. Hennawi et al. 2006; Myers et al. 2008) is much larger than that in our sample, a direct comparison with other results is at present not possible. For instance, the extended sample of QSO pairs of Hennawi et al. (2006) covers a wide redshift range (up to $z=3$, majority of pairs at $z>1$), for which a detailed environmental study is not available and would require a major observational effort on large telescopes. Recently Green et al. (2011) studied the environments around 7 close QSO pairs ($R_{\perp} < 30$ kpc) in a redshift range comparable with ours. They searched for extended X-ray emission as evidence for a local group - or cluster - sized dark matter halo associated with these quasar pairs, and found none. In potential contrast to our results, they didn't detect a significant optical/infrared galaxy density enhancement. Moreover, due to the relatively bright magnitude limits of SDSS images at the redshift of these pairs, only the most luminous galaxies possibly associated to the quasars could be detected using their DWCM technique (Distance and error-Weighted Color Mean, Green et al. 2011). Within these limits, their results that QSO pairs avoid rich cluster environments are qualitatively in agreement with our findings.

Since the environment around pairs is relatively poor, it is of interest to compare it with the minimum mass of the binary system (the two QSOs) assuming it is gravitationally bound. Following F11 we computed the minimum virial mass associated to each pair and compared it with the total mass of the host galaxies (see Table 3), evaluated following Kotilainen et al. (2009) and Decarli et al. (2010). While in most cases the $M_{vir,min}$ is less or similar than the total mass of the host galaxies, in 3 cases (out of 14) $M_{vir,min}$ exceeds the sum of the masses of the hosts by a factor $\gtrsim 10$ (see Table 5). This is suggestive of a huge dark matter contribution (see also F11). However, because of the exiguity of our sample, to reach a firm conclusion on the environment and dynamical properties of QSO pairs, a detailed spectroscopic

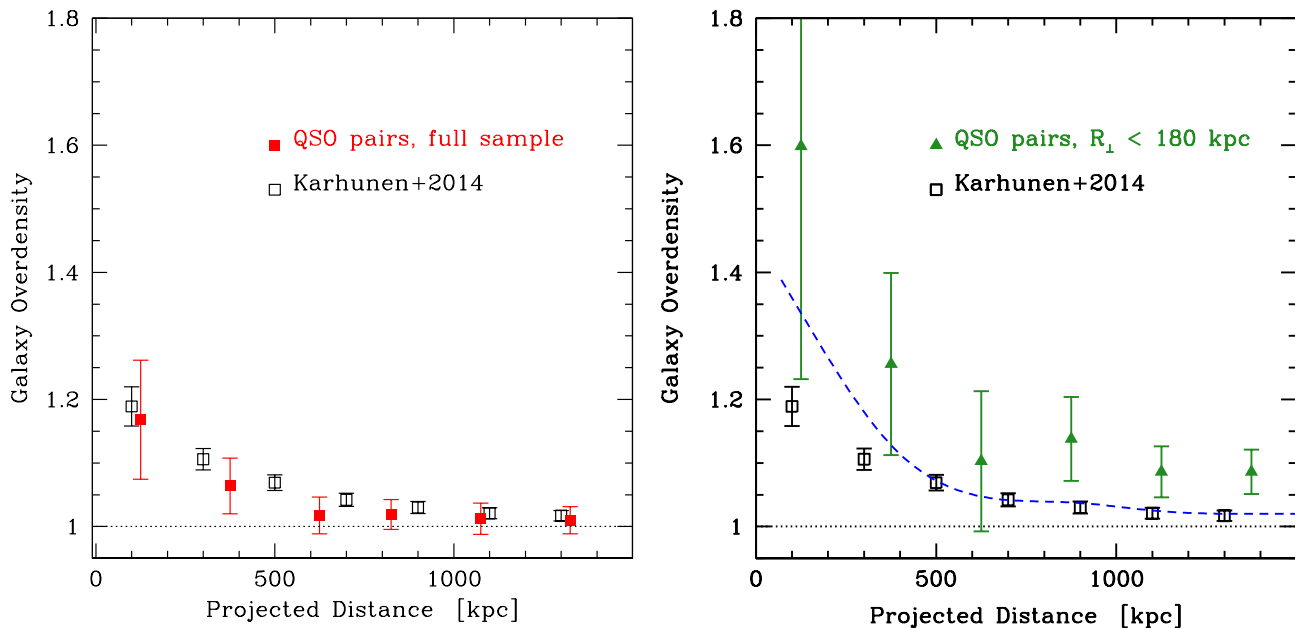


Figure 4. *Left panel:* SDSS i-band mean cumulative overdensity of galaxies around the quasars in pairs, corrected for the superposition of the companion environment (red filled squares) as a function of the projected distance from the quasars. *Right panel:* Same as left panel for whole QSO pairs with $0 < R_{\perp} < 180$ kpc (green full triangles). The expected galaxy overdensity around the whole QSO pairs, derived from the galaxy overdensity in the left panel is plotted with the blue dashed line. In both the panels the mean cumulative overdensity around isolated quasars from the subsample at $i < 22$ mag derived by Karhunen et al. (2014) is plotted for a comparison.

Table 5. Comparison of the minimum virial mass of the the QSO pairs with the total mass of their host galaxies.

Pair Nr	$M_{vir,min}$ [$10^{12} M_{\odot}$]	$M_{host,A} + M_{host,B}$ [$10^{12} M_{\odot}$]
(a)	(b)	(c)
1	(0.03 ± 0.09)	0.4
2	(0.05 ± 0.10)	1.1
3	0.20 ± 0.06	1.2
4	(0.13 ± 0.12)	0.6
5	1.9 ± 0.2	1.0
6	20 ± 4	0.6
7	0.7 ± 0.2	(1.7)
8	25 ± 2	1.2
9	1.1 ± 0.3	(1.0)
10	8 ± 1	2.4
11	(0.00 ± 0.02)	(1.1)
12	(0.14 ± 0.22)	2.0
13	0.30 ± 0.04	(1.8)
14	12 ± 2	0.6

(a) Quasar pair identification number. (b) Minimum virial mass of the binary system. Values encompassed by bracket are not enough constrain. (c) Total mass of the QSO host galaxies in the pair. In the cases where only one quasar is resolved (see Table 3; in brackets), we consider as the total mass the twice of the resolved quasar.

and imaging investigation of a larger and homogeneous sample is required.

ACKNOWLEDGMENTS

We thank the referee for her/his constructive report which enable us to improve our paper.

We acknowledge the support of the Italian Ministry of Education (grant PRIN-MIUR 2010-2011).

EPF acknowledges funding through the ERC grant Cosmic Dawn.

Funding for the creation and distribution of the SDSS Archive has been provided by the Alfred P. Sloan Foundation, the Participating Institutions, the National Science Foundation, the U.S. Department of Energy, the National Aeronautics and Space Administration, the Japanese Monbukagakusho, the Max Planck Society, and the Higher Education Funding Council for England. The SDSS Web Site is <http://www.sdss.org/>.

REFERENCES

- Bennert, N., Canalizo, G., Jungwiert, B., et al. 2008, ApJ, 677, 846
 Boris N. V., Sodr e L., Jr., Cypriano E. S., Santos W. A., de Oliveira C. M., West M., 2007, ApJ, 666, 747
 Callegari, S., Kazantzidis, S., Mayer, L., et al 2011, ApJ, 729, 85
 Capak P., et al., 2007, ApJS, 172, 99
 Croom S. M., et al., 2005, MNRAS, 356, 415

- Decarli R., Falomo R., Treves A., Kotilainen J. K., Labita M., Scarpa R., 2010, MNRAS, 402, 2441
- Di Matteo T., Springel V., Hernquist L., 2005, Natur, 433, 604
- Djorgovski S., Perley R., Meylan G., McCarthy P., 1987, ApJ, 321, L17
- Djorgovski S., 1991, ASPC, 21, 349
- Djorgovski S. G., Courbin F., Meylan G., Sluse D., Thompson D., Mahabal A., Glikman E., 2007, ApJ, 662, L1
- Ellingson, E., Yee, H. K. C., & Green, R. F. 1991, ApJ, 371, 49
- Falomo R., Bettoni D., Karhunen K., Kotilainen J. K., Uslenghi M., 2014, MNRAS, 440, 476
- Farina E. P., Falomo R., Treves A., 2011, MNRAS, 415, 3163
- Farina E. P., Montuori C., Decarli R., Fumagalli M., 2013, MNRAS, 431, 1019
- Fisher, K. B., Bahcall, J. N., Kirhakos, S. & Schneider, D. P. 1996, ApJ, 468, 469
- Francis P. J., Drake C. L., Whiting M. T., Drinkwater M. J., Webster R. L., 2001, PASA, 18, 2
- Green P. J., Myers A. D., Barkhouse W. A., Aldcroft T. L., Trichas M., Richards G. T., Ruiz Á., Hopkins P. F., 2011, ApJ, 743, 81
- Hennawi J. F., et al., 2006, AJ, 131, 1
- Hennawi J. F., et al., 2010, ApJ, 719, 1672
- Hewett P. C., Wild V., 2010, MNRAS, 405, 2302
- Karhunen K., Kotilainen J. K., Falomo R., Bettoni D., 2014, arXiv, arXiv:1404.1642
- Kormendy, J., Fisher, D. B., Cornell, M. E. & Bender, R. 2009, ApJS, 182, 216
- Kotilainen J. K., Falomo R., Decarli R., Treves A., Uslenghi M., Scarpa R., 2009, ApJ, 703, 1663
- Liu X., Shen Y., Bian F., Loeb A., Tremaine S., 2013, arXiv, arXiv:1312.6694
- Mannucci F., Basile F., Poggianti B. M., Cimatti A., Daddi E., Pozzetti L., Vanzi L., 2001, MNRAS, 326, 745
- McIntosh, D. H., Guo, Y., Hertzberg, J., et al. 2008, MNRAS, 388, 1537
- McLure, R. J., Dunlop, J. S. 2001, MNRAS, 321, 515
- Myers A. D., Richards G. T., Brunner R. J., Schneider D. P., Strand N. E., Hall P. B., Blomquist J. A., York D. G., 2008, ApJ, 678, 635
- Pâris I., et al., 2013, arXiv, arXiv:1311.4870
- Porciani C., Magliocchetti M., Norberg P., 2004, MNRAS, 355, 1010
- Schneider D. P., et al., 2010, AJ, 139, 2360
- Serber W., Bahcall N., Ménard B., Richards G., 2006, ApJ, 643, 68
- Silk J., Wyse R. F. G., 1993, PhR, 231, 293
- Stockton, A. 1978, ApJ, 223, 747
- Uslenghi M., Falomo R., 2008, mss.conf, 313
- Veron-Cetty M.-P., Veron P., 2000, cqaan.book,
- Wake D. A., et al., 2004, ApJ, 610, L85
- Yee, H. K. C. & Green, R. F. 1984, ApJ, 280, 79
- Yee, H. K. C. & Green, R. F. 1987, ApJ, 319, 28
- Zhdanov V. I., Surdej J., 2001, A&A, 372, 1